

[Chem. Pharm. Bull.]
33(4)1633-1640(1985)]

The Behavior of 1,4-Benzodiazepine Drugs in Acidic Media. II.¹⁾ Kinetics and Mechanism of the Acid-Base Equilibrium Reaction of Oxazolam

YUKIHISA KURONO,*^a TOMONARI KUWAYAMA,^b KINYA KAMIYA,^a
TAMOTSU YASHIRO,^a and KEN IKEDA^a

Faculty of Pharmaceutical Sciences, Nagoya City University,^a 3-1
Tanabe-dori, Mizuho-ku, Nagoya 467, Japan and Pharmacy,
Tokai Teishin Hospital,^b 2-17-5 Matsubara,
Naka-ku, Nagoya 460, Japan

(Received July 9, 1984)

The oxazolidine ring-opening and ring-closing reactions (acid-base equilibrium reactions) of oxazolam were investigated by using a stopped-flow spectrophotometer. The *cis* and *trans* isomers of oxazolam were found to have distinct ring-opening rate constants and the constant of the *cis* isomer was 10 to 20 times larger than that of the *trans* isomer. The ring-opening is hydrogen ion-catalyzed at low pH region. The ring-closing occurs in a hydroxide ion-catalyzed reaction in the alkaline region and is affected by the deprotonation of the diazepinone ring. The individual intrinsic rate constants for the ring-opening and ring-closing reactions were determined from the rate-pH profile. These rate measurements are of value to distinguish between *cis* and *trans* isomers of oxazolam.

Keywords—oxazolam; benzodiazepinooxazole; *cis-trans* isomer; kinetics; equilibrium reaction; stopped-flow spectrophotometer; rapid scan spectrophotometer; NMR spectrum

It is of importance to examine the chemical structure and stability of drug species in the physiological pH range. Ikeda and Nagai investigated the acid-base equilibrium reactions of benzodiazepinooxazoles (oxazolidine ring-opening and ring-closing reactions) and determined the equilibrium constants.²⁾ They also studied the kinetics and mechanism of hydrolysis of the diazepinone ring of oxazolam.³⁾ We previously investigated the structural changes of some benzodiazepinooxazoles in acid solution using ¹H- and ¹³C-nuclear magnetic resonance (NMR) spectroscopy.¹⁾ In order to understand fully the stability of oxazolam in aqueous solution, the present study deals with the kinetics and mechanism of oxazolidine ring-opening and ring-closing reactions of oxazolam by using the stopped-flow method.

Experimental

Materials and Apparatus—Oxazolam was a gift from Sankyo Co., Ltd. (lot 8) and was used without further purification. The ratio of *cis* to *trans* isomers was about 2:3.^{4,5)} All other chemicals were obtained commercially and were of reagent grade.

Ultraviolet (UV) absorption spectra were obtained on a Hitachi UV-124 spectrophotometer and a Union Giken rapid-scan spectrophotometer (RA-415). A Union Giken stopped-flow spectrophotometer (RA-401) was used for the measurement of the reaction rates. ¹H-NMR spectra were obtained in a JNM-FX 100 spectrometer using tetramethylsilane as an internal standard. A Hitachi-Horiba F-7_{LC} pH meter was employed for pH measurement.

Determination of p*K*_a—The p*K*_a value of oxazolam was determined spectrophotometrically based on Eq. 1.⁶⁾

$$\log \frac{A - A_B}{A_A - A} = pK_a - pH \quad (1)$$

In Eq. 1, A_A , A_B and A are the absorbances at an appropriate wavelength for the acid form, base form, and their mixture, respectively. When A_B could not be measured experimentally, the following equation was employed for the determination of the K_a value.

$$\frac{1}{A - A_A} = \frac{1}{K_a (\epsilon_B [D]_T - A_A)} [H^+] + \frac{1}{\epsilon_B [D]_T - A_A} \quad (2)$$

where ϵ_B and $[D]_T$ are the molar absorbance ($M^{-1} \text{ cm}^{-1}$) of the base form of oxazolam and the total concentration of oxazolam, respectively. The K_a value can be obtained from the intercept divided by the slope of the plot of $1/(A - A_A)$ versus $[H^+]$ based on Eq. 2.

Kinetic Runs—The buffer systems used were as follows: below pH 1.0, an appropriate concentration of hydrochloric acid; pH 2.0–3.5, 0.20 M glycine-HCl; pH 4.0–5.5, 0.20 M acetate; pH 6.0–7.5, 0.067 M phosphate; pH 8.0–9.0, 0.05 M borate–0.10 M phosphate; pH 10–11, 0.05 M borate–0.05 M carbonate; pH 12.0, 0.20 M borate–0.10 M NaOH; pH 12.5, 0.10 M glycine–0.10 M NaOH; above pH 13, an appropriate concentration of sodium hydroxide.

All the experiments except for the $^1\text{H-NMR}$ measurement of oxazolam were carried out at 25°C in aqueous buffer containing 5% (v/v) ethanol with $\mu = 0.2 \text{ M}$ (KCl). A stock solution of oxazolam ($6.4 \times 10^{-4} \text{ M}$) was prepared in ethanol, and when required, a solution was also prepared in methanol or dimethylformamide. A 2 ml aliquot of the stock solution was diluted to 20 ml with 0.002 M glycine-HCl buffer of pH about 3 or 0.0005 M borate–0.001 M phosphate buffer of pH about 9. One syringe of the stopped-flow instrument was filled with this solution, while the other syringe contained an appropriate concentration of buffer. It was found preliminarily that the desired pH buffers could be obtained on mixing of equal volumes of these two solutions. The ring-opening reaction was started by the rapid mixing of the diluted buffer (pH about 9) containing oxazolam and the appropriate acid buffer. The reaction was followed by monitoring the increase in absorbance at 240 nm. The ring-closing reaction was initiated by the mixing of the diluted buffer (pH about 3) containing oxazolam and the appropriate alkaline buffer, and was followed by recording the decrease in absorbance at 240 nm. The data of successive measurements on the same reaction mixture were accumulated at least 5 times to enhance the signal-to-noise ratio. The pseudo-first-order rate constant (k_{obs}) was calculated from the slope of a linear plot of $\log(A_t - A_\infty)$ versus time, where A_t and A_∞ are the absorbance readings at time t and at infinity when no further absorbance changes occurred, respectively. When A_∞ was unknown, the Guggenheim method⁷⁾ was applied for the determination of the rate constant. These analyses of the data were made directly by using a Sord microcomputer (M223 Mark III) linked to the stopped-flow instrument.

The UV absorption spectra of the ring-opening reaction were measured with the rapid-scan spectrophotometer. The rate constant for the reaction was also estimated by analysis of the spectra, for comparison with that from the stopped-flow analysis.

Results and Discussion

Acid-Base Equilibrium Reaction of Oxazolam

The UV spectra of oxazolam in various pH buffer solutions are shown in Fig. 1(a). It has been reported¹⁻³⁾ that the spectra below pH 9.0 (Fig. 1(a)) correspond to those of equilibrium mixtures of the ring-opened iminium form (AF) in acid solution and the ring-closed form (BF) in neutral to weak alkaline solution. Each structure of oxazolam is shown in Chart 1. Figure 1(b) shows the plot of absorbance at 240 nm versus pH. For the reaction ($\text{AF} \rightleftharpoons \text{BF} + \text{H}^+$), the apparent $\text{p}K_{a,1}$ value ($-\log([\text{BF}][\text{H}^+]/[\text{AF}])$) was estimated from the data in Fig. 1(b) by using Eq. 1. The value obtained was 5.5, which is in agreement with the literature values (5.6²⁾ and 5.3⁸⁾). Above pH 12, further absorbance changes were observed as shown in Fig. 1(b). These changes are considered to be due to the deprotonation of the diazepinone ring of oxazolam (BI), as reported for 1,4-benzodiazepines.^{8,9)} The $K_{a,2}$ value ($[\text{BI}][\text{H}^+]/[\text{BF}]$) was estimated by using Eq. 2, and was found to be $3.16 \times 10^{-13} \text{ M}$. This value agrees fairly with that ($1.26 \times 10^{-12} \text{ M}$) in the literature⁸⁾ and is comparable with those of 1,4-benzodiazepines.⁹⁾

The ring-closing reaction (initiated by a pH-jump, for example, from pH 3.1 to 9.1) proceeded in a single step, as shown in Fig. 2, and followed first-order kinetics. On the other hand, the ring-opening reaction (e.g., pH-jump from pH 8.9 to 3.1) occurred in two steps, as shown in Fig. 2. The sum of the increments of the absorbances due to the fast step and the slow step (i.e., total absorbance increment shown in Fig. 2) is essentially the same as the increment of the absorbance calculated from the static spectra (shown in Fig. 1(b)) of oxazolam in the corresponding pH buffers (pH 8.9 and 3.1). Both the fast and slow steps

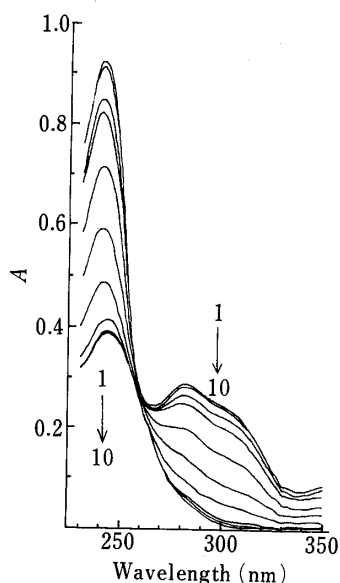


Fig. 1(a). UV Absorption Spectra of Oxazolam in Buffers with Various pH Values

Concentration of oxazolam, 3.2×10^{-5} M.
1, pH 1.44; 2, 3.12; 3, 4.08; 4, 5.01; 5, 5.53; 6, 6.02;
7, 6.54; 8, 6.69; 9, 8.08; 10, 8.96.

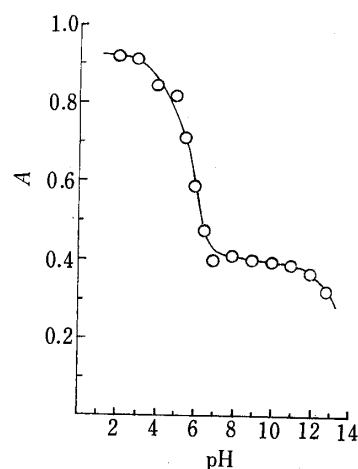


Fig. 1(b). Plot of Absorbance at 240 nm versus pH

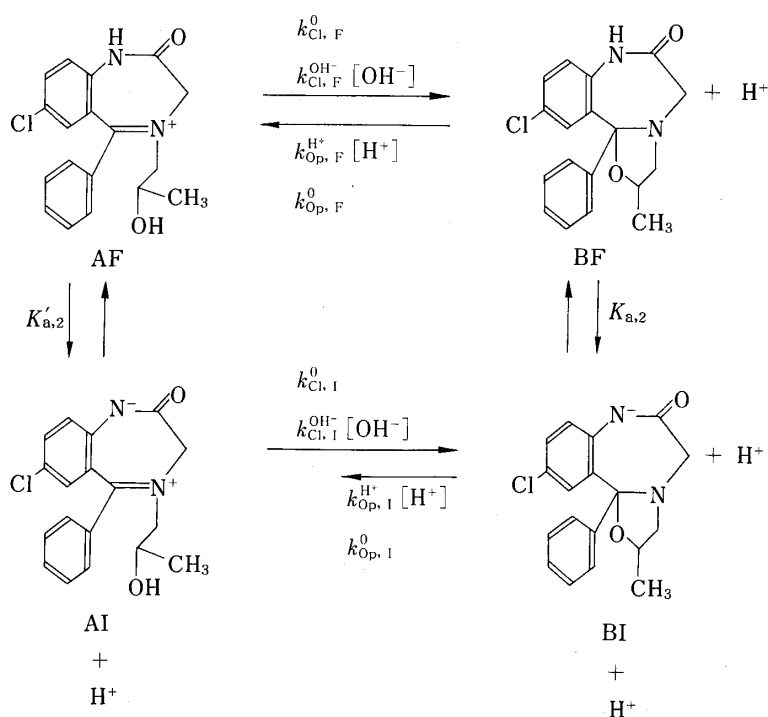


Chart 1

individually followed first-order kinetics.

To clarify the nature of the two step reactions the rapid-scan spectra were measured, and are shown in Figs. 3(a) and 3(b). Both spectra in Figs. 3(a) and 3(b) show isosbestic points at about 255 nm. The absorbance increases simply with time on both sides of 255 nm. These spectral changes with time are similar to those with pH shown in Fig. 1(a). The pseudo-first-order rate constants estimated from the spectra in Figs. 3(a) and 3(b) are identical with those calculated from the absorbance change in Fig. 2. The two reactions, therefore, cannot be

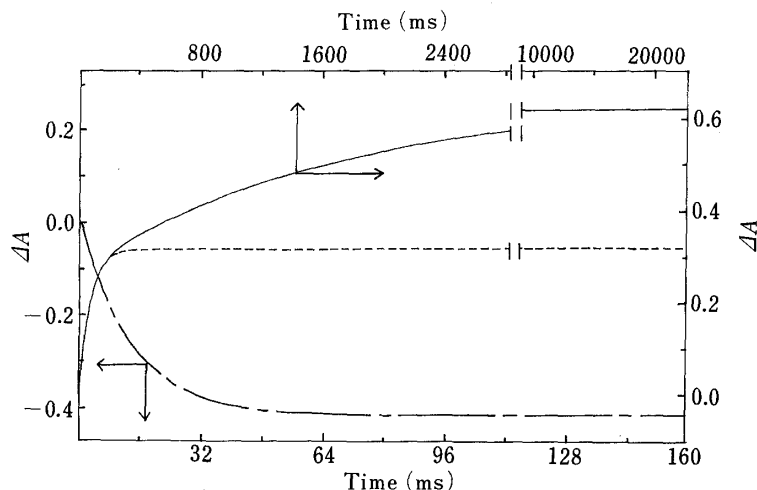


Fig. 2. Absorbance Changes with Time Due to the Ring-Opening and Ring-Closing Reactions at 25 °C

---, ring-closing reaction initiated by pH-jump from pH 3.1 to 9.1; —, ring-opening reaction initiated by pH-jump from pH 8.9 to 3.1; - - - - , simulated curve assuming the fast ring-opening reaction alone, where ΔA_{∞} was estimated by Guggenheim analysis.⁷⁾

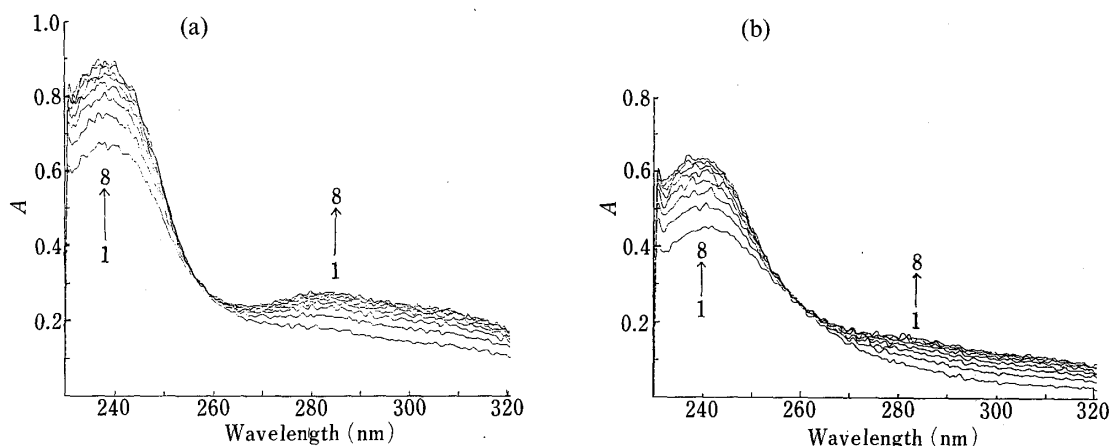


Fig. 3. Rapid-Scan Spectra for the Ring-Opening Reaction Initiated by pH-Jump from pH 8.9 to 3.1 at 25 °C

- (a) Fast (1st) step.
1, 17 ms; 2, 37; 3, 57; 4, 77; 5, 97; 6, 117; 7, 137; 8, 157.
- (b) Slow (2nd) step.
1, 327 ms; 2, 927; 3, 1527; 4, 2127; 5, 2727; 6, 3327; 7, 3927; 8, 4527.

characterized individually from the static UV absorption spectra alone, but have different rate constants (one is 10 to 20 times larger than the other).

It has been reported^{4,5,10)} that oxazolam exists as a mixture of *cis* and *trans* isomers (nearly 2:3, respectively) in chloroform and dimethylformamide, the structures being as shown in Chart 2. The terms *cis* and *trans* refer to the 2-methyl group and 11b-phenyl group. To confirm the existence of the isomers in the aqueous buffer containing 5% (v/v) ethanol, the ¹H-NMR spectra of oxazolam in D₂O and/or ethanol-*d*₆ were measured. Oxazolam was, however, practically insoluble in D₂O and the methyl signal of oxazolam in the spectrum overlapped with that of ethanol-*d*₆. Moreover, the kinetic results obtained using the stock solution of oxazolam in methanol were found preliminarily to be almost identical with those in ethanol. Consequently, methanol-*d*₄ was used as the solvent of oxazolam for the ¹H-NMR measurement. The ¹H-NMR spectrum of oxazolam in methanol-*d*₄ is shown in Fig. 4. Two

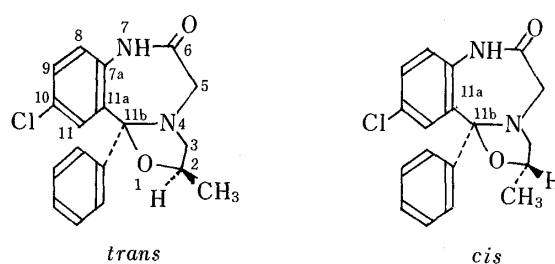


Chart 2

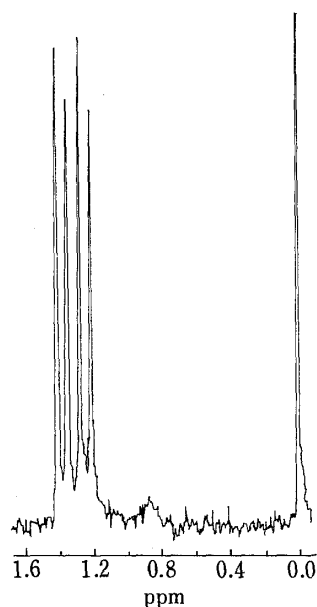


Fig. 4. $^1\text{H-NMR}$ Spectrum (100 MHz) of an Equilibrium Mixture of *cis*- and *trans*-Oxazolam in Methanol- d_4

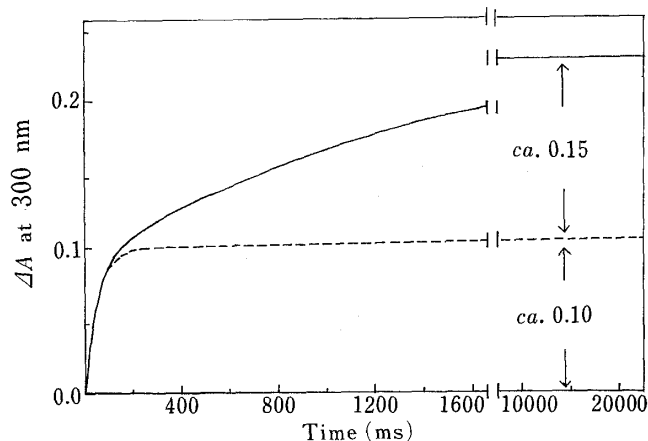


Fig. 5. Absorbance Changes with Time in the Ring-Opening Reaction Using Stock Solution Prepared in Dimethylformamide

—, ring-opening reaction initiated by pH-jump from pH 8.9 to 3.1; ----, simulated curve assuming *cis* isomer ring-opening reaction alone, where ΔA_∞ was estimated by Guggenheim analysis.⁷⁾

The stock solution was used at about 3 h after preparation. Absorbance change was measured at 300 nm, because 5% (v/v) dimethylformamide solution has a considerable absorbance at 240 nm.

methyl proton doublets (each $J=6.5$ Hz) are observed at 1.24 and 1.36 ppm, which are almost the same positions as those in chloroform and dimethylformamide.^{4,5)} The *cis/trans* isomer ratio obtained by integrating the signals was about 1. The two step reactions shown in Figs. 2 and 3, therefore, can be attributed to these isomers having different ring-opening rate constants.

In order to determine which reaction is faster, the stock solution of oxazolam in dimethylformamide was employed for the measurement of the ring-opening rates of the *cis* and *trans* isomers. The ratio of the absorbance increment of the fast step to that of the slow step was about 2:3, as shown in Fig. 5. In dimethylformamide, as reported in the literature,^{4,5,10)} the ratio of *cis* to *trans* isomers is nearly 2:3. The fast reaction, therefore, can be considered to be due to the *cis* isomer of oxazolam and the slow one to the *trans* isomer.

Although there is no experimental evidence, the reason for the ring opening rate difference between *cis* and *trans* isomers may be as follows. Sato *et al.*¹¹⁾ reported that in the crystal structure of the 10-bromo analog of *trans*-oxazolam, the lone pair of the nitrogen atom at position 4 is directed towards the same side as the phenyl group attached to the carbon atom at position 11b (conformation I). Using the CPK model, another conformation for oxazolam can be considered, in which the lone pair of the nitrogen atom occupies the opposite side to the phenyl group (conformation II). It is probable that oxazolam dissolved in the aqueous solution would exist in both conformations, and the conversion rate between

conformations I and II might be very large. An approach of a proton to the lone pair of the nitrogen atom is necessary for the oxazolidine ring-opening reaction. Proton approach to the lone pair may occur mainly in conformation II, because in conformation I the steric hindrance by the 11b-phenyl group is very large. In conformation II, the steric hindrance by the 2-methyl group of the *trans* isomer (the 2-methyl and 11b-phenyl groups are *trans*) is larger than that by the 2-methyl group of the *cis* isomer, since in the *trans* isomer the lone pair and 2-methyl group exist on the same side of the oxazolidine ring plane. Proton approach to the lone pair in the *trans* isomer is, therefore, more difficult than that in the *cis* isomer, and the ring-opening of the *cis* isomer is faster than that of the *trans* isomer. This speculation requires experimental confirmation.

pH Profile of Equilibrium Rate Constant of Oxazolam

Figure 6 shows the pH-rate profile for the acid-base equilibrium reactions of oxazolam. The effect of the buffer constituents on the rate was found preliminarily to be small, so that the k_{obs} value without correction for the buffer effect is used for this profile. The two profiles in the acid region are due to *cis* and *trans* isomers as described above. There is a minimum point in the weak acid region and a sigmoidal portion is seen in the alkaline region. The reaction scheme shown in Chart 1 can account for this profile. The rate constant $k_{\text{Cl,F}}^0$ represents the water-catalyzed ring-closing reaction from the free form (AF) of nitrogen at the 7 position, and $k_{\text{Cl,F}}^{\text{OH}^-}$ is the hydroxide ion-catalyzed ring-closing rate constant. The rate constant $k_{\text{Cl,I}}^0$ represents the water-catalyzed ring-closing reaction from the ionic form (AI), and $k_{\text{Cl,I}}^{\text{OH}^-}$ is the hydroxide ion-catalyzed ring-closing rate constant. The constant $k_{\text{Op,F}}^{\text{H}^+}$ is the hydrogen ion catalyzed ring-opening rate constant from the free form (BF) of nitrogen at the 7 position, and $k_{\text{Op,F}}^0$ is the water-catalyzed ring-opening rate constant from BF. The rate constant $k_{\text{Op,I}}^{\text{H}^+}$ represents the hydrogen ion-catalyzed ring-opening reaction from the ionic form (BI), and $k_{\text{Op,I}}^0$ is the water-catalyzed ring-opening rate constant from BI. $K_{\text{a},2}$ and $K'_{\text{a},2}$ are the dissociation constants of BF and AF, respectively.

It is assumed that the equilibria defined by $K_{\text{a},2}$ and $K'_{\text{a},2}$ in Chart 1 are much faster than the processes of ring-opening and ring-closing.¹²⁾ The reactions defined by $k_{\text{Op,I}}^{\text{H}^+}$ and $k_{\text{Op,I}}^0$ cannot be measured, because when the pH is jumped from the alkaline region to the acid region, BF is formed instantaneously by acceptance of H^+ , and ring-opening of BF occurs.

According to Chart 1, k_{obs} below pH 8¹³⁾ in Fig. 6 is given by Eq. 3.

$$k_{\text{obs}} = k_{\text{Op,F}}^{\text{H}^+}[\text{H}^+] + k_{\text{Op,F}}^0 + k_{\text{Cl,F}}^0 + k_{\text{Cl,F}}^{\text{OH}^-}[\text{OH}^-] \quad (3)$$

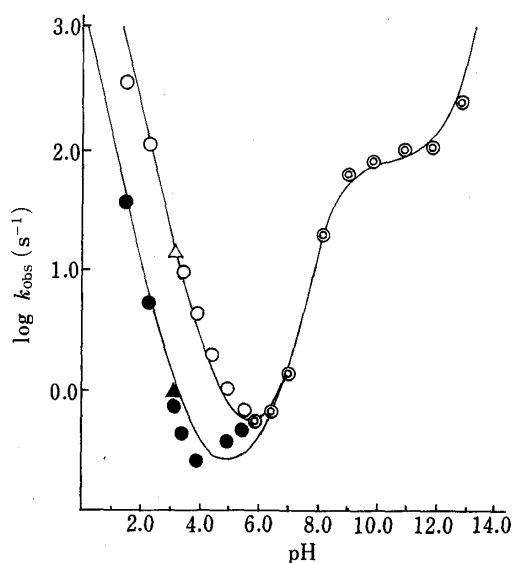


Fig. 6. The pH-Rate Profiles for Oxazolidine Ring-Opening and Ring-Closing Reactions of Oxazolam at 25°C

○, reaction of the *cis* isomer initiated by pH-jump from alkaline to acid region; ●, reaction of the *trans* isomer initiated by pH-jump from alkaline to acid region; ⊙, reaction initiated by pH-jump from acid to alkaline region; △, reaction of the *cis* isomer using the stock solution in methanol; ▲, reaction of the *trans* isomer using the stock solution in methanol.

TABLE I. Estimated Rate Constants and Dissociation Constants^{a)}

$k_{\text{Op,F}}^{\text{H}^+}$ $\text{s}^{-1} \text{M}^{-1}$	$k_{\text{Op,F}}^0 + k_{\text{Cl,F}}^0$ s^{-1}	$k_{\text{Cl,F}}^{\text{OH}^-}$ $\text{s}^{-1} \text{M}^{-1}$	$k_{\text{Cl,I}}^0$ s^{-1}	$k_{\text{Cl,I}}^{\text{OH}^-}$ $\text{s}^{-1} \text{M}^{-1}$	$K'_{\text{a,2}}$ M	$K_{\text{a,2}}$ M
<i>cis</i> isomer						
2.08×10^4	5.58×10^{-1}		1.31×10^7	2.75×10	3.88×10^3	1.95×10^{-9}
						3.16×10^{-13}
<i>trans</i> isomer						
1.19×10^3	1.97×10^{-1}					

a) Temperature, 25 °C; containing 5% (v/v) ethanol.

The $k_{\text{Op,F}}^{\text{H}^+}$ and $k_{\text{Cl,F}}^{\text{OH}^-}$ values can be estimated from the k_{obs} values at the regions having slopes of -1 and $+1$ in the profile, respectively. The obtained values are listed in Table I. Since the $k_{\text{Op,F}}^0$ and $k_{\text{Cl,F}}^0$ values cannot be calculated individually, their sum ($k_{\text{Op,F}}^0 + k_{\text{Cl,F}}^0$) was calculated near the minimum portion of k_{obs} by using Eq. 4.

$$k_{\text{Op,F}}^0 + k_{\text{Cl,F}}^0 = k_{\text{obs}} - (k_{\text{Op,F}}^{\text{H}^+}[\text{H}^+] + k_{\text{Cl,F}}^{\text{OH}^-}[\text{OH}^-]) \quad (4)$$

The values obtained are also included in Table I.

Above pH 8¹³⁾ the k_{obs} value is given by Eq. 5.

$$k_{\text{obs}} = (k_{\text{Cl,F}}^0 + k_{\text{Cl,F}}^{\text{OH}^-}[\text{OH}^-])f_{\text{AF}} + (k_{\text{Cl,I}}^0 + k_{\text{Cl,I}}^{\text{OH}^-}[\text{OH}^-])f_{\text{AI}} \\ = \frac{1}{[\text{H}^+] + K'_{\text{a,2}}} \{k_{\text{Cl,F}}^0[\text{H}^+] + k_{\text{Cl,F}}^{\text{OH}^-}K_{\text{w}} + k_{\text{Cl,I}}^0K'_{\text{a,2}} + k_{\text{Cl,I}}^{\text{OH}^-}(K_{\text{w}}/[\text{H}^+])K'_{\text{a,2}}\} \quad (5)$$

where f_{AF} and f_{AI} are the molar fractions of AF and AI, respectively. K_{w} is the ionic product of water and is assumed to be $1 \times 10^{-14} \text{M}^2$. On the assumption that at pH 9–10 the predominant term in Eq. 5 is $k_{\text{Cl,F}}^{\text{OH}^-}$ alone, an approximate $K'_{\text{a,2}}$ value was calculated by using the equation $k_{\text{obs}} = k_{\text{Cl,F}}^{\text{OH}^-}K_{\text{w}}/([\text{H}^+] + K'_{\text{a,2}})$. The $k_{\text{Cl,I}}^{\text{OH}^-}$ value was estimated from the region of $K'_{\text{a,2}} \gg [\text{H}^+]$. Furthermore the $k_{\text{Cl,I}}^0$ value was estimated by using $k_{\text{Cl,F}}^{\text{OH}^-}$, $K'_{\text{a,2}}$, $k_{\text{Cl,I}}^{\text{OH}^-}$ (which are determined already) and k_{obs} . The values thus obtained are listed in Table I. The solid lines depicted in Fig. 6 were calculated by applying the values in Table I to an equation which was obtained easily by the rearrangement (*i.e.*, combination) of Eqs. 3 and 5. The observed data points fit well to the calculated lines.

The minimum point of the profile is calculated as follows. Differentiating k_{obs} in Eq. 3 with respect to $[\text{H}^+]$ gives Eq. 6.

$$\frac{dk_{\text{obs}}}{d[\text{H}^+]} = \frac{k_{\text{Op,F}}^{\text{H}^+}[\text{H}^+]^2 - k_{\text{Cl,F}}^{\text{OH}^-}K_{\text{w}}}{[\text{H}^+]^2} \quad (6)$$

When the value of $dk_{\text{obs}}/d[\text{H}^+]$ is zero, the profile should be minimum. The hydrogen ion concentration at the minimum point, $[\text{H}^+]_{\text{min}}$, is expressed by Eq. 7.

$$[\text{H}^+]_{\text{min}} = (k_{\text{Cl,F}}^{\text{OH}^-}K_{\text{w}}/k_{\text{Op,F}}^{\text{H}^+})^{1/2} \quad (7)$$

Substituting the numerical values into Eq. 7 gives the results $[\text{H}^+]_{\text{min}} = 2.51 \times 10^{-6} \text{M}$ and $1.05 \times 10^{-5} \text{M}$, and thus $\text{pH}_{\text{min}} = 5.60$ and 4.98 , respectively. The calculated pH_{min} 's are almost identical with the observed pH_{min} 's in Fig. 6.

The $K'_{\text{a,2}}$ value ($1.95 \times 10^{-9} \text{M}$) is rather large compared with the $K_{\text{a,2}}$ value ($3.16 \times 10^{-13} \text{M}$) of oxazolam and those of 1,4-benzodiazepines.^{8,9)} This large $K'_{\text{a,2}}$ may be explained as follows. AI may have a resonance structure (AI') in which the electric charges are neutralized, as shown in Chart 3. This resonance structure may facilitate deprotonation from AF compared with that from BF. This structure (AI'), moreover, may explain the large

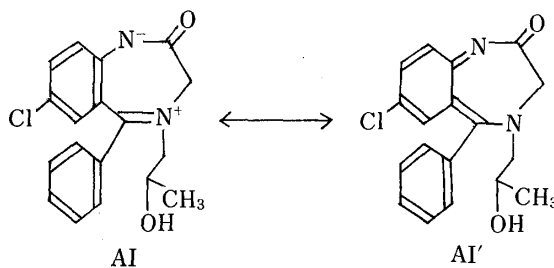


Chart 3

difference between $k_{\text{Cl,F}}^{\text{OH}^-}$ and $k_{\text{Cl,I}}^{\text{OH}^-}$ ($k_{\text{Cl,F}}^{\text{OH}^-} = 3 \times 10^3 k_{\text{Cl,I}}^{\text{OH}^-}$). The intramolecular nucleophilic attack of the neighboring hydroxyl group to the iminium carbon may be retarded by this resonance structure.

In conclusion, this rate measurement by stopped-flow spectrophotometry is a valuable method to distinguish between the *cis* and *trans* isomers of oxazolam, although this method alone cannot determine which isomer reacts faster than the other. The ability to observe ring-opening rates for both *cis*- and *trans*-oxazolam implies that the rates of ring-opening are faster than the rate of *cis-trans* isomerization of oxazolam. Furthermore, this study suggests that from a pharmacological point of view the stereochemistry (*cis* or *trans*) of crystal oxazolam may be unimportant when oxazolam administered orally is dissolved in the stomach and adsorbed in the intestine. The *cis*- and/or *trans*-oxazolam form a common quaternary iminium ion (AF in Chart 1) in the stomach (*i.e.*, in an acid environment) and then in the intestine (*i.e.*, in a neutral or weak alkaline environment). AF forms *cis*- and *trans*-oxazolam in equal proportions.¹⁴⁾

Acknowledgement The authors are grateful to Miss. S. Kato of this university for NMR measurement. Thanks are also due to Sankyo Co., Ltd. for a gift of oxazolam.

References and Notes

- 1) Part I: T. Kuwayama and T. Yashiro, *Yakugaku Zasshi*, **104**, 607 (1984).
- 2) M. Ikeda and T. Nagai, *Chem. Pharm. Bull.*, **30**, 3810 (1982).
- 3) M. Ikeda and T. Nagai, *Chem. Pharm. Bull.*, **32**, 1080 (1984).
- 4) T. Miyadera, A. Terada, M. Fukunaga, Y. Kuwano, T. Kamioka, C. Tamura, H. Takagi, and R. Tachikawa, *J. Med. Chem.*, **14**, 520 (1971).
- 5) T. Miyadera, A. Terada, C. Tamura, M. Yoshimoto, and R. Tachikawa, *Ann. Rep. Sankyo Res. Lab.*, **28**, 1 (1976).
- 6) Y. Kurono, K. Ikeda, K. Uekama, *Chem. Pharm. Bull.*, **23**, 340 (1975).
- 7) E. A. Guggenheim, *Phil. Mag.*, **2**, 538 (1926); A. A. Frost and R. G. Pearson "Kinetics and Mechanism," 2nd ed., Wiley International Edition, New York, 1961, p. 49.
- 8) E. Graf and M. El-Menshawey, *Pharmazie in Unserer Zeit*, **6**, 171 (1977).
- 9) J. Barrett, W. F. Smith, and I. E. Davidson, *J. Pharm. Pharmacol.*, **25**, 387 (1973).
- 10) M. E. Derieg, J. V. Earley, R. I. Fryer, R. J. Lopresti, R. M. Schweiniger, L. H. Sternbach, and H. Wharton, *Tetrahedron*, **27**, 2591 (1971).
- 11) S. Sato, N. Sakurai, T. Miyadera, C. Tamura, and R. Tachikawa, *Chem. Pharm. Bull.*, **19**, 2501 (1971).
- 12) The assumption is based on the fact that the rate of deprotonation (proton dissociation) of barbiturates was too fast to measure with our stopped-flow spectrophotometer (data not shown).
- 13) This pH value was chosen on the basis of the $\text{p}K_{\text{a},1}$ and $\text{p}K'_{\text{a},2}$ values.
- 14) This phenomenon was confirmed *in vitro* as follows. An aliquot (4 ml) of the oxazolam stock solution in ethanol was diluted to 25 ml with 0.001 M HCl solution; the pH value of the solution was about 3.1 (the molecular species is AF). Then 10 ml of the acid solution was diluted to 25 ml with the diluted buffer (pH about 9); the pH value of this solution was about 7.0 (the molecular species is BF). The dilute neutral solution was mixed with the appropriate acid buffer (pH 3.0) in the stopped-flow apparatus. The reactions proceeded in two steps, similar to those in Fig. 2, and the ratio of the absorbance increment due to the *cis* isomer to that due to the *trans* isomer was approximately 1.